RECONSTRUCTION OF THE VERTICAL STRUCTURE OF INTERNAL WAVES IN THE TROPOSPHERE FROM MULTIFREQUENCY MEASUREMENTS IN THE O_2 LINES

K P. Gaikovich and A. V. Troitskii

UDC 551.575:551.543:551.521.9

The observed frequencies of internal gravity waves (IGWs) and their contribution to the variability of the brightness temperatures were determined on the basis of spectral analysis of the temporal dynamics of the thermal radio emission of the atmosphere at the frequencies 53.5, 54.0, 54.5, and 55.0 GHz. Methods for reconstructing from multifrequency measurements in the O-, lines the altitude distribution of the perturbation of the temperature of IGWs from the spectral amplitudes of their contribution to the brightness temperature were developed.

1. Internal Gravity Waves in the Boundary Layer of the Atmosphere. The sources of IGWs are atmospheric fronts, mesoscale processes, obstacles in the path of wind (mountains), storms, as well as tectonic processes. Internal gravity waves can propagate virtually undamped in a stably stratified layer of air over large distances from sources (hundreds and thousands of kilometers) and in the process transport significant energy.

In a stably stratified layer, i.e., when the temperature gradient $\gamma = dT/dz$ satisfies the condition $\gamma > \gamma_a$, where $\gamma_a = —9.8$ Km is (he adiabatic gradient, the equation for the vertical velocity of the particles of IGWs have the following form in the Boussinesq approximation

$$\frac{\partial^2}{\partial z^2} \Delta W + N^2 \Delta_\perp W = 0, \tag{1}$$

where

$$N^2 = -\frac{g}{\rho}\frac{\partial \rho}{\partial z} = \frac{g}{T}(\gamma - \gamma_a). \tag{2}$$

Here N is the Brunt—Vaisala frequency, which usually ranges from several to tens of minutes, g is the acceleration of gravity, p is the density of air, and T is the temperature. Internal gravity waves with frequencies $\omega \le N$ and vertical scale comparable to the thickness of the stable layer propagate. Under conditions of waveguide propagation above the earth's surface, the solution of Eq. (1) for the amplitude of the fundamental mode

$$W = W_0 \sin \frac{\pi}{\Delta z} z, \tag{3}$$

where Δz is the thickness of the stable layer of the atmosphere, corresponds to zero boundary conditions for the stable layer. The process of wave oscillations in the IGWs is nearly adiabatic, i.e., displacement of some volume of air by the amount Δz changes its temperature by the amount $\Delta T = \gamma_a \Delta z$, while the temperature at the level z, to which this volume was displaced, changes by the amount $\Delta T = (\gamma_a — \gamma)\Delta z$. For $\Delta z = 100$ m the quantity ΔT can be equal to several degrees; this makes it possible to observe temperature oscillations in IGWs from the corresponding measurements of the thermal radio emission of the atmosphere in the absorption lines of O_2 with resonances at the wavelengths $\lambda = 5$ mm and $\lambda = 2.6$ mm. By observing IGWs with frequency ω it is easy to obtain from Eq. (3), assigning that the vertical scale of the oscillations is less than Δz, an expression for the vertical profile of the amplitude of the periodic disturbance of the temperature:

$$\Delta T(z) = \frac{W_0}{\omega}\left(\gamma_a - \gamma\right) \sin \frac{\pi}{\Delta z} z. \tag{4}$$

Scientific-Research Radiophysical Institute. Translated from Izvestiya Vysshikh Uchebnykh Zavedenii, Radioftzika, Vol. 34, No. 2, pp. 103-110, February, 1991. Original article submitted November 3, 1989.

0033-8443/91/3402-0089S12.50

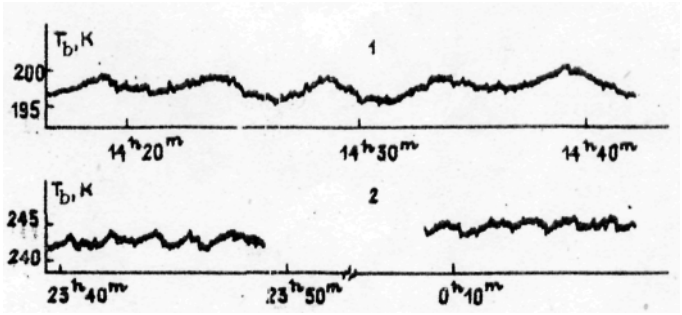

Fig. 1

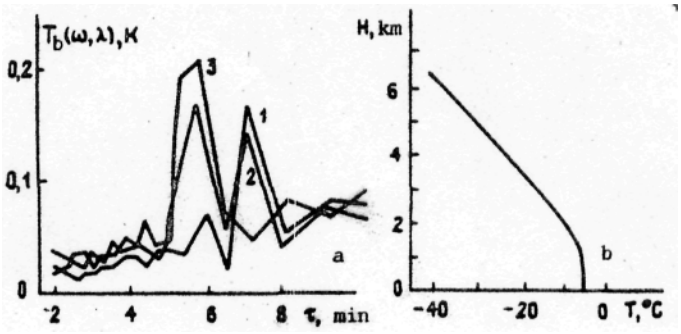

Fig. 2

The periods of HGWs are usually equal to several minutes and the wavelengths are equal to several kilometers. In the real atmosphere the distribution $\Delta T(z)$ can be more complicated than Eq. (4), because of the possible alt ii ude dependence of the temperature gradient, as well as in cases when the disturbance is strong, which results in breaking of waves and appearance of cellular circulation, which makes the problem multidimensional.

2. Variations of the Thermal Radio Emission of the Atmosphere Accompanying Propagation of IGWs. The expression for the brightness temperature of thermal radio emission of the atmosphere in ground-based measurements at wavelength λ and in the direction with zenith angle θ has the form

$$T_b(\lambda,\theta)=\frac{1}{\cos\theta}\int_0^\infty T(z)\kappa(z,\lambda)\exp\left(-\frac{1}{\cos\theta}\int_0^z\kappa(z',\lambda)dz'\right)dz=\int_0^\infty T(z)K(\lambda,z)dz, \quad (5)$$

where $\kappa(z,\lambda)$ is the absorption coefficient.

It is well known that the altitude profile $T(z)$ can be reconstructed from elevation-angle or spectral measurements in the O_2 lines on the basis of the solution of a Fredholm integral equation of the first kind (5) [2, 3]. Physically, the solution is based on the fact that the thickness of the layer in which the radiation is formed depends on the wavelength and elevation angle of observation while the intensity of the radiation is proportional to the air temperature. It should be noted that although Eq. (5) is improperly-posed and it requires the use of additional a priori information about the properties of the exact solution, it has been demonstrated that it is possible to reconstruct the characteristic features of the distribution $T(z)$ in the boundary layer of air, including inversion situations [3], when propagation of IGWs is especially likely. In principle, the variations of $T(z)$ in IGWs can be reconstructed directly from measurements of T_b at a series of wavelengths or the dependence $T_b(\theta)$. However, the amplitude of the oscillations of T_b usually does not exceed several tens of degrees Kelvin, which is comparable to the level of the fluctuation sensitivity of a radiometer (~0.3 K with integration constant $\tau = 4$ sec). Sometimes, though rarely, cases of strong oscillations of T_b are encountered; such oscillations were recorded in the first observations of IGWs |4].

Figure 1 shows examples of observations of IGWs at the frequency 53.5 GHz (1 — case of isothermal stratification ($\gamma \approx 0$ K/km); 2 — inversion stratification ($\gamma = 50$ K/km)]. In order to detect most IGWs, however, the sensitivity must be high; detection is also hindered by turbulent fluctuations of the thermal radio emission, which can also be of the same order of magnitude as the effect owing to the presence of the wave process itself. It is difficult to increase the sensitivity by increasing the integration time,

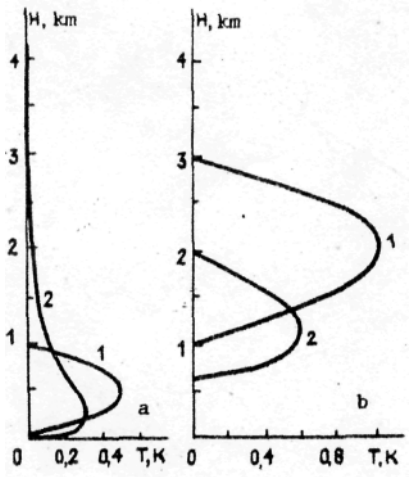

Fig. 3

since the period of the IGW is not known beforehand. An effective method in this case could be spectral analysis of the observed dynamics of $T_b(t)$, which, when a periodic component is present in T_b, makes it possible to separate this component reliably against the background of the wide spectrum of turbulent fluctuations of the radiation and the radiometer noise. An independent analysis of the dynamics of T_b at different wavelengths makes it possible to increase the significance of the detection of IGWs, and it also makes it possible to reconstruct the altitude distribution of the amplitude of the oscillations of $T(z)$ on the basis of the solution of the corresponding inverse problem. At the same time, the stratification of the temperature, according to which it is possible to estimate the conditions of propagation of the observed IGWs, can be reconstructed from the solution of the problem for the constant component of T_b. The elevation-angle method of reconstructing IGWs is limited, because of the need to perform measurements in the direction along the azimuth, perpendicular to the direction of propagation of an IGW. The idea of detecting IGWs on the basis of spectral analysis of measurements was used in |5|. But there the dependence $T_b(t)$ was regarded as a random process, and the autocorrelation function and the power spectrum of T_b were detected (the latter by Fourier transforming the former). The power spectrum of T_b makes it possible to judge the presence of a wave process, but this physical characteristic is not simply related with the altitude distribution of the temperature perturbation, and this made it impossible, in spite of the existence of multifrequency measurements, for the authors to make further progress in the problem of detecting IGWs and to reconstruct the altitude structure of the temperature oscillations.

By studying the Fourier expansion of the time dependence $T_b(t)$ itself it is possible to obtain an equation relating the corresponding components of this expansion with the components of the Fourier expansion of $T(z,t)$. We have

$$T_b(\lambda,t) = \int_0^\infty T(z,t)K(\lambda,z)dz = \sum_{i=1}^{\infty} T_b(\omega_i,\lambda)\cos(i\omega t) + T_b^0(\lambda), \tag{6}$$

where $\omega_j = i\omega$ and $T_b°(\lambda)$ is the constant component of T_b. Analogously, we represent $T(z,t)$ in the form

$$T(z,t) = \sum_{i=1}^{\infty} T(\omega_i,z)\cos(i\omega t) + T^0(z). \tag{7}$$

The components $T_b(\omega_j, \lambda)$ are determined from

$$T_b(\omega_i,\lambda) = \int_0^{\pi/\omega} T_b(\lambda,t)\cos(i\omega t)dt, \quad i = 0,1,2,\ldots \tag{8}$$

The time interval $t_m = \pi/\omega$ in which the function is expanded is chosen to be long enough so that $\omega \ll N$ and the terms in the series (6) will contain harmonics which are known to be close to the frequency N. Then, obviously,

$$T_b(\omega_i,\lambda) = \int_0^\infty T(\omega_i,z)K(\lambda,z)dz, \tag{9}$$

TABLE 1

ν, GHz		53.5	54	54.5	55
$T_B(\omega_1)$	$\theta = 0$	0.08	0.12	0.16	0.2
	$\theta = 76^0$	0.26	0.28	0.3	0.26
$T_B(\omega_2)$	$\theta = 0$	0.16	0.18	0.15	0.06

which is the analog of Eq. (5) for the spectral components of T_b and T(z). For the constant components we have

$$T_b^0(\lambda) = \int_0^\infty T^0(z)K(\lambda)dz. \tag{10}$$

It is possible to formulate on the basis of Eqs. (9) and (10) the problem of determining the spectral amplitude of IGWs $T(\omega_i,z)$ and the stratification $T°(z)$. whence the distribution $T(z,t)$ itself can be easily reconstructed from Eq. (7). In me process, the Fourier analysis was performed over a period of 64 min with a time step of 30 sec.

Figure 2a shows the results of the spectral analysis of the dynamics of brightness temperatures at the frequencies 53.5, 54.5, and 55 GHz (curves 1-3; $\tau = 2\pi/\omega$), while Fig. 2b shows the corresponding distribution $T°(z)$, obtained by solving Eq.(10) by the method of statistical regularization (maximum entropy) analogously to [3] using *a priori* information about the multilevel covariation matrix of the temperature B_{TT}. One can see that in the case presented in Fig. 2b there exist layers for which the necessary condition for propagation of IGWs $\gamma > \gamma_a$ is satisfied. Indeed, there exists a layer, extending from the earth's surface up to ~1 km, where the distribution $T°(z)$ is close to the isothermal distribution ($\gamma = 0$). At higher altitudes $z > 1$ km the gradient $\gamma = —6$ K/km. Since $\gamma > \gamma_a$, we can sec that a wave process, but with a different characteristic frequency, is also possible in this layer. Estimates-of the Brunt-Vaisala frequencies N from Eq. (2) give $N_1 = 0.019$ sec^{-1} for the layer near the ground and $N_2 = 0.0126$ sec^{-1} in the second layer, respectively; these values are in good agreement with the frequencies of the maxima of the spectral amplitudes of T_b in Fig. 2a ($\omega_1 = 0.018$ sec^{-1} and $\omega_1 = 0.014$ sec^{-1}) and shows that the observed spectral characteristics are indeed related with IGWs. Spectral analysis of the brightness temperatures did not reveal any features during absolute calibration with respect to reference standards; this eliminates the possibility of interpreting the observed effect as a manifestation of periodic variations of the gain of the radiometer. The level of the spectral amplitudes of the noise in the process of calibration as well as at frequencies outside the observed maxima gives an estimate of the error δT_b of the right-hand side of Eq. (9), which was employed to reconstruct the corresponding harmonics of the perturbation of the temperature profile. From Fig. 2a it is evident that $\delta T_b = 0.01$-0.03 K. The spectral amplitudes $T_b(\omega, \lambda)$ for the data in Fig. 2 are presented in Table 1.

3. Reconstruction of the Amplitude Profile of the Temperature Perturbation in IGWs from Multifrequency Radiometric Measurements. The problem of reconstructing the spectral amplitude $T(\omega_i,z)$ from Eq. (9) is equivalent in form to the problem of reconstructing the constant component T°(z) from Eq. (10). For compactness, we rewrite both equations in operator form:

$$\begin{aligned} KT &= T_b^\delta, \\ KT &= \int_0^\infty T(z)\, K(z,\lambda)\, dz, \end{aligned} \tag{11}$$

where T_b^δ is the measured realization of the right-hand side, whose error δT_b satisfies the inequality

$$\delta^2 T_b = \| KT - T_b^\delta \|_{L_2}^2 = \int_{\lambda_1}^{\lambda_2} [T_b(\lambda) - T_b^\delta(\lambda)]^2 d\lambda, \tag{12}$$

and $T_b(\lambda)$ corresponds to the exact solution $T(z)$. In order to solve Eq. (11) it is necessary to use not the exact kernel K but rather an approximate kernel K_h, whose measure of error h is estimated as

$$h = \sup \frac{\|KT - K_h T\|}{\|T\|} \tag{13}$$

This is because the problem is formulated in a discrete form when it is solved numerically and because the kernel K is nonlinear owing to the weak temperature dependence of the absorption coefficient of the radio waves. It should also be noted that the smoothing

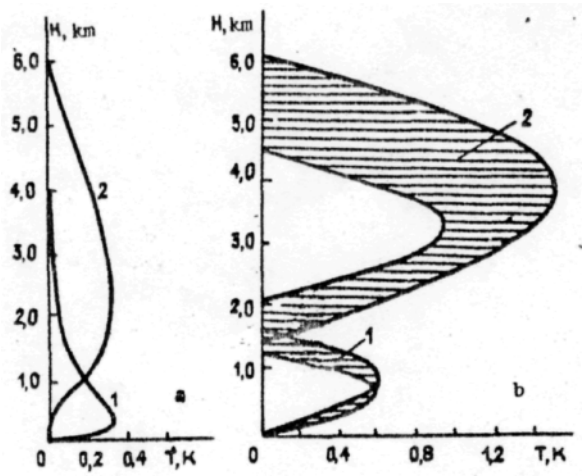

Fig. 4

effect of the kernel limits the class of possible realizations of $T_b(\lambda)$, and when the function T_b^{δ} contains a random error it can fall outside the admissible class, and this makes Eq. (11) incompatible. The measure of incompatibility then satisfies

$$\mu = \inf \|K_h T - T_b^{\delta}\|. \tag{14}$$

Obviously,

$$\mu \leq \delta T_b + h\|T\|. \tag{15}$$

Equation (11) is a Fredholm integral equation of the first kind. It is well known that the solution of such equations is an improperly posed problem, i.e., when solving Eq. (11) without the use of adequate additional a priori information about the form of the distribution $T(z)$ small errors δT_b correspond to arbitrarily large errors in $T(z)$. This means that the operator inverse to the completely continuous operator K is unbounded. The choice of the specific algorithm for solving Eq. (11) depends on the form of the a priori information employed. Unfortunately, the equation for the periodic component cannot be solved using statistical information about its average value and the covariation function, as is successfully done for the constant component, for which there exist extensive aerological data for most climatic conditions. For this reason, in order to solve the problem Tikhonov's method was employed in the form of the principle of generalized discrepancy, which employs information about the smoothness of the exact solution |6]. The possibilities of using this method for radiometric sounding of temperature profiles in the boundary layer were studied in |7].

According to (6], in order to find the approximate solution of Eq. (11) it is necessary to minimize on the set of differentiable functions the functional

$$M^{\alpha}(t) = \|K_h T - T_b^{\delta}\|_{L_2}^2 + \alpha\|T\|_{W_2^1}^2 = \int_{\lambda_2}^{\lambda_1}\left[\int_0^{\infty} K_h(\lambda, z)T(z)dz - T_b^{\delta}(\lambda)\right]^2 d\lambda + \alpha\int_0^{\infty}\left[T^2(z) + \left(\frac{dT}{dz}(z)\right)^2\right]dz, \tag{16}$$

where ||x|| designates the norm of the function x as an element of the space L_2 or W_2^1 (definitions are given in [6]). It was shown in [6] that if the regularization parameter is matched with the error of measurements in a definite manner, in particular if it is defined as the root of the one-dimensional nonlinear equation for the generalized discrepancy

$$\rho(\alpha) = \|K_h T^{\alpha} - T_b^{\delta}\|_{L_2}^2 - (\delta T_b + h\|T^{\alpha}\|)^2 - \mu^2 = 0, \tag{17}$$

where $\|T\|_{W_2^1}^2 = \int_0^{\infty}(|T(z)|^2 + |T'(z)|^2)dz$, then as $\delta T_b \to 0$ the approximate solution T^{α} approaches uniformly the exact solution $T(z)$. This is a big advantage of the method under study over most other methods, whose solutions cannot, as a rule, be shown to converge. The convex functional (16) is minimized by gradient methods, which have been well studied from the computational tandpoint of the problem of quadratic programming. The measure of discrepancy μ is determined in the process of minimizing (17) and for the problem at hand usually $\mu << \delta T_b$. The measure of error of the kernel h is also found by means of a numerical

experiment. In this case h is determined by the nonlinearity associated with the temperature of the kernel K, and for different functions $T(z)$ the corresponding error $h\|T\|$ in Eq. (17) ranges from 10^{-6} to $3\cdot10^{-2}$ K.

The method also permits flexible use of additional information about the exact solution $T(z)$ in the form of constraints, if it is known that the exact solution is greater (or less) than some function or if the function is finite and its carrier is known. A more accurate solution can be obtained if the solution can be sought as a deviation from an "average" model or "probable" distribution.

When solving an improperly posed problem it is possible to establish universally valid relations between the error of measurement and the error of reconstruction. It is necessary to perform a numerical experiment using a closed scheme; this makes it possible to judge the quality of the reconstruction for the class of exact solutions studied and for the type of errors studied, and it also makes it possible to choose the optimal measurement parameters (set of wavelengths and their number).

In the case at hand the altitude range in which perturbations $T(z)$ arc possible can be judged from the profile of the constant component $T°(z)$. The condition that $T(z)$ is nonnegative can be used as additional information. Numerical experiments (see Fig. 3a) have shown that for distributions of the type (4) with an amplitude of 0.5 K and measurement accuracy δT_b = 0.01-0.03 K the reconstructed profiles arc close to the starting profiles; the error of determination of the amplitude is equal to -0.2 K. Analogous disturbances at altitudes above 1 km (Fig. 3b) are not reconstructed as well and require higher accuracy (~ 0.015 K); such accuracy already falls at the level of error $h\|T\|$, introduced by the temperature dependence of the kernel (in Fig. 3 the curves 1 represent the starting profiles and the curves 2 represent the reconstructed profiles). The number of wavelengths employed is fully adequate for the existing level of error, but when sounding the layer 0-1 km it is best to choose their values closer to the resonance of the oxygen spectrum or to perform oblique measurements at angles $\theta \approx 70\text{-}80°$. The results once again agree with the results obtained in the case studied in [7|, which is physically close to our case.

The problem analyzed here can be solved by an alternative approach, since the exact theoretical form of the altitude distribution of the amplitude of the IGWs (4) is known though, of course, it should be kept in mind that the assumptions incorporated in the derivation of (4) arc satisfied only approximately in the real atmosphere. Nonetheless, substituting Eq. (4) into Eq. (9), it is possible to obtain a system of equations at different wavelengths for the parameters of the sinusoidal perturbation. We rewrite Eq. (4) in the form

$$T(z) = A \sin\left(\pi \frac{z - h_0}{\Delta h}\right), \qquad h \le z \le h_0 + \Delta h \tag{18}$$

taking into account the possibility of the existence of IGWs in the layer $h_0 < z < h_0 + \Delta h$. Then ihe corresponding system of equations assumes the form

$$T_b(\lambda_n) = \int_0^\infty A \sin\left(\pi \frac{z - h_0}{\Delta h}\right) K(\lambda_n, z)\, dz. \tag{19}$$

In order to determine the three unknown parameters (18) it is formally sufficient to have observations at three wavelengths. Since errors are present, it is also helpful to use a large number of wavelengths and, for example, the method of least squares. Since The integral in Eq. (19) cannot be determined analytically, the corresponding problem was solved numerically by running through values of the parameters A, h_0, and Δh in the intervals 0.1-2 K, 0-2 km, and 0.5-4 km, respectively, with steps of 0.1 K, 0.1 K/km, and 0.1 km, respectively. The solutions were the functions (18) satisfying the conditions

$$T_b(\lambda_n) \le \delta T_R, \qquad n = 1 - 4. \tag{20}$$

4. Results of Reconstruction. The results of reconstruction of the profiles of the amplitudes of temperature oscillations in IGWs by the two methods studied above are presented in Fig. 4 (a — reconstruction by Tikhonov's method; b — family of solutions (hatched regions), satisfying Eq. (20) for the model (18)]. It is evident from these results that the wave processes at two different frequencies ω_1 and ω_2 are indeed localized in different altitude layers and their characteristic scales agree with the structure of the constant component of the temperature profile T°(z) (see Fig. 2b). In the layer 0-1 km there exists a process with a characteristic period λ_1 = 350 sec. The altitude distributions of the amplitudes of the oscillations in this layer, reconstructed by the two different methods, closely coincide with one another (see Fig. 4a, b, curves 1).

A wave process also exists in the layer above 1 km, but its characteristic period is different: λ_2 = 450 sec, which corresponds to a different temperature gradient. As already mentioned above, the accuracy of the reconstruction for the same level of errors of measurement decreases with altitude, so that the reconstruction by the two methods reveals a large spread of values. However, both methods agree in that the process is located primarily at altitudes above 1 km (see Fig. 4a, b, curves 2). It should be noted

that the purely sinusoidal process of the type (18) can he made to agree with measurements based on (20), setting δT_b not less than 0.06 K, while Tikhonov's method gives a solution with a more realistic estimate $\delta T_b = 0.03$ K. There are grounds for supposing that in the layer 1-6 km the process is not sinusoidal, since the air density decreases significantly with increasing altitude, and this is not taken into account in the derivation of Eq. (3).

The amplitudes of the oscillations of the vertical velocity and the displacement of air in IGWs, described by the relation (3), can be estimated from the amplitudes of the temperature oscillations using Eq. (4). For the layer 0-1 km, $W_0 = T_{max}\omega/(\gamma_a - \gamma) = 1.1$ m/sec and the displacement amplitude $A = w_0/\omega = 60$ m. In the layer 1-6 km, correspondingly, $W_0 = 3.2$ m/sec and $A = 250$ m.

The estimates agree with the characteristic parameters of the IGWs.

The obtained results show that multifrequency radiometric measurements can be used to observe and determine the vertical structure and parameters of IGWs, even in complicated cases when the process exists simultaneously in different altitude intervals.

LITERATURE CITED

1 . L. M. Brekhovskikh and V. V. Goncharov, *Introduction to the Mechanics of Continuous Media* [in Russian), Nauka, Moscow.

2. V. 1. Aleshin, A. P. Naumov, et al., *Izv. Vyssh. Uchebn. Zaved., Radiofiz.,* **20**, No. 2, 193 (1977).

3. A. V. Troitskii, *Izv. Vyssh. Uchebn. Zaved,, Radiofiz.,* **26**, No. 8, 878 (1986).

4. A. V. Troitskii, in: Abstracts of Reports at the AH-Union Symposium on the Propagation of Millimeter and Submillimeter Waves in the Atmosphere. Frunze (1986), p. 139.

5. M. EI-Raeys, *Radio Sci.,* **17**, No. 14, 766 (1982).

6. A. N. Tikhonov, A. V. Goncharskii, ct al,, *Reclamation Algorithms and a priori Information* (in Russian], Nauka, Moscow (1983).

7. K. P. Gaikovich and M. I. Sumin, in: Abstracts of Reports at the All-Union Conference on Radio Meteorology, Moscow (1986), p.6.